Available online at www.sciencedirect.com
SCIENCE DIRECT®
Peptides 24 (2003) 679–685
PEPTIDES
www.elsevier.com/locate/peptides

Humanin peptides block calcium influx of rat hippocampal neurons by altering fibrogenesis of $A\beta_{1-40}$

Ping Zou, Yanan Ding, Yinlin Sha*, Baihe Hu, Songqing Nie

Single Molecule and Nano-biomedicine Laboratory, Department of Biophysics, Peking University School of Basic Medical Sciences, Biochemistry Building 204#, Xueyuan Road 38#, Beijing 100083, China

Received 12 December 2002; accepted 7 April 2003

Abstract

Humanin peptides (including HN, HNG and other mutants) were reported previously that antagonize neurotoxicity caused by various familial Alzheimer's disease (FAD) genes and Aβ derivatives. Herein, we describe the aggregation dynamics and the representative morphological characteristics of $A\beta_{1-40}$ after different time of addition humanin peptides, which revealed that (a) the interactions of both HN and HNG with $A\beta_{1-40}$ induced quick and significant increase of light-scattering intensity, and (b) HNG also caused obvious morphological alteration from fibrillary to amorphous. In the meantime, the experiments also revealed that the interaction of HNG with $A\beta_{1-40}$ could decrease $A\beta_{1-40}$-induced calcium rise, an initial event accompanying $A\beta_{1-40}$-induced apoptosis of cultured neurons. Our results indicate that HNG can protect neurons by altering $A\beta_{1-40}$ morphology.

Keywords: Humanin; Electron microscopy; Aβ aggregation; Calcium influx; Neurotoxicity

1. Introduction

Alzheimer's disease (AD), characterized by synaptic loss, neuronal death in cerebral cortex and hippocampus, and the presence of extensive extracellular amyloid plaques and intracellular neurofibrillary tangles [19], represents the most common cause of dementia of the elderly population whose incidence doubles every 5 years between 65 and 85 years old [13]. The amyloid cascade hypothesis of AD pathology proposed that the neurodegeneration observed in AD brains is best explained as a series of events triggered by the abnormal processing of the amyloid precursor protein (APP), the consequences of which are the production, aggregation, deposition and neurotoxicity of Aβ derivatives [6]. Aβ derivatives are major protein component of the amyloid plaque and are present mainly in two forms, $A\beta_{1-40}$ and $A\beta_{1-42}$. Although $A\beta_{1-42}$ seems to be the pathogenic species in early-onset familiar AD, increased deposition of $A\beta_{1-40}$ is characteristic in late-onset AD bearing the apoE4 allele (apoE4), a susceptibility factor for late-onset AD [5]. In addition, $A\beta_{1-40}$ is the most prevalent form present in brain, blood vessels, and other tissues derived from AD and normal [20]. Since Aβ self-assembles accompanied by conformational transition in solution, AD was usually termed as a protein "conformational disease" defined by Carrell and Lomas [3]. Although the mechanism of Aβ fibrogenesis is not clear yet, it is usually suggested that amyloid fibrils formation is an ordered polymerization process characterized by slow nucleation, followed by rapid growth step [7,15]. Understanding Aβ self-assembly process and Aβ-induced multiple events in culture is important not only for clarifying AD, but also for considering neuron protective approaches.

Despite some clinical trials with encouraging results, no curative therapy for this disease has so far been developed. Recently, Nishimoto and coworkers [9–11] found that a series of peptides termed humanin peptides could effectively abolish neuronal cell death by a wide spectrum of familial Alzheimer's disease (FAD) genes and Aβ derivative. The wild-type humanin (HN) was coded by a gene screening from the occipital lobe of the AD brain, as they reasoned that protective genes must be expressed in neurons in the

Abbreviations: HN, wild-type humanin MAPRGFSCLL LLTSEIDLPV KRRA; HNG, humanin peptide mutant Ser14Gly; TEM, transmission electron microscopy; SEM, scanning electron microscopy; HPLC, high performance liquid chromatography; Fmoc, 9-fluorenylmethoxycarbonyl; HBTU, 2-(1*H*-benzotriazol-1-yl)-1,1,3,3-tetramethyl uranium hexafluorophosphate; TFA, trifluoroacetic acid; HOBT, 1-hydroxybenzotrizole; MALDI-TOF MS, matrix assist laser desorption ionization-time of flying mass spectrometry; Aβ, β-amyloid peptide

* Corresponding author. Tel.: +86-10-8233-2096; fax: +86-10-8233-2096.
E-mail address: shyl@bjmu.edu.cn (Y. Sha).

0196-9781/$ – see front matter © 2003 Elsevier Inc. All rights reserved.
doi:10.1016/S0196-9781(03)00131-1

occipital lobe of the AD brain, which is well known to be maintained intact throughout the course of this devastating disease [9]. It is interesting to note that a S14G mutant (HNG) resulted in 1000 times potentiation of the action of HN and is fully active at low nanomolar concentrations [9].

To further reveal relationships between humanin peptides and $A\beta_{1–40}$ fibrogenesis accompanied by neurotoxicity, we investigated the interactions between humanin peptides and $A\beta_{1–40}$ and found that the HNG interaction with $A\beta_{1–40}$ could decrease $A\beta_{1–40}$-induced calcium entry into neurons, a primary $A\beta_{1–40}$-induced event following with neurotoxicity in culture [1,18].

2. Materials and methods

2.1. Peptide synthesis and purification

The sequences of HN and its S14G mutant (HNG) list as follows [11]:

MAPRGFSCLL LLTS EIDLPV KRRA (HN)

MAPRGFSCLL LLTG EIDLPV KRRA (HNG)

HN and HNG amide were prepared by solid phase peptide synthesis strategy, Fmoc chemistry [4]. Rink resin, 2-(1*H*-benzotriazol-1-yl)-1,1,3,3-tetramethyl uranium hexafluorophosphate (HBTU), 1-hydroxybenzotrizole (HOBT) and 9-fluorenylmethoxycarbonyl amino acids FmocMet, FmocAla, FmocPro, FmocArg(pdf), FmocGly, FmocPhe, FmocSer(Bu^t), FmocCys(trt), FmocLeu, FmocThr, FmocGlu(OBu^t), FmocIle, FmocAsp(OBu^t) and FmocVal were utilized. The peptides resin were cleavaged using Reagent K (5% phenol/5% thioanisole/2.5% 1,2-ethanedithiol/5% H_2O/82.5% TFA) [4]. The crude peptides were purified by high performance liquid chromatography (HPLC) and the final products were confirmed using matrix assist laser desorption ionization-time of flying mass spectrometry (MALDI-TOF MS) ([M + H], HN: observed 2686.9/calculated 2685.6; HNG: observed 2655.3/calculated 2655.6). The HN and HNG solution in PBSA (27 mM KCl, 137 mM NaCl, 0.02% NaN_3, pH 7.2), at 10 mg/ml were filtered through 0.22 μm filters and were stored at −20 °C.

2.2. $A\beta_{1–40}$ peptide

$A\beta_{1–40}$ (DAEFRHDSGY EVHHQKLVFF AEDVGSNKGA IIGLMVGGVV) was purchased from AnaSpec, Inc. (San Jose, CA), confirmed using MALDI-TOF MS (calculated 4330.9/observed 4331.0) and HPLC (>95%). $A\beta_{1–40}$ was treated for 1 h with 100% trifluoroacetic acid (TFA) at room temperature and the exceeding TFA was removed under a stream of nitrogen until a clear film remained in the test tube [22], so as to obtain chemical homogeneous sample. The pretreated $A\beta_{1–40}$ was then dissolved in DMSO at 10 mg/ml and stored at −20 °C.

2.3. Light scattering

The dynamic process of aggregation of $A\beta_{1–40}$ + HN (molar ratio, 1:2), $A\beta_{1–40}$ + HNG (molar ratio, 1:2) and $A\beta_{1–40}$, were investigated using light-scattering function of Hitachi 4500 fluorescence spectrophotometer. All the three samples were dissolved in PBSA at pH 7.2, and the final concentration of $A\beta_{1–40}$ in all samples was 100 μM. Samples were transferred quickly into clean light-scattering cuvettes equipped with a temperature-controlled (37 °C) bath after a brief vortex. Data were collected at 488 nm, at each after 24 h during 12 days.

2.4. Electron microscopy (EM)

Transmission electron micrographs were acquired using JEM-1230 performed with an accelerating voltage of 80 kV. A 7 μl sample was placed on a Formvar-coated grid. After 10 min, the grids were blotted and the samples were stained with 1% phosphotungstic acid solution. Scanning electron micrographs were taken by JEM-5600LV. After centrifugation at 16,000 × *g* for 10 min, discarded the supernatant, the samples were washed with distilled water to removing salts. After that, the samples were dotted on holders and were coated with gold with ion-sprayer after drying.

2.5. Hippocampal neuron primary cultures [2]

Hippocampi were obtained from postnatal rats (<1 day) and incubated for 15 min in Hank's balanced salts solution (HBSS) containing 2.5 μg/ml trypsin. The hippocampi were then rinsed three times in 10 ml of DMEM (5 g/l *N*-(2-hydroxyethyl) piperazine-*N*′-(2-ethanesulfonic acid) (HEPES), 3.7 g/l sodium bicarbonate, 0.3 g/l glutamine and 10 mg/ml gentamicin, pH 7.2) containing 10% (v/v) heat-inactivated fetal bovine serum (FBS, Gibco). After that, cells were dissociated by trituration using narrowed bore of a fire-polished Pasteur pipette and were distributed to the Peri-culture dishes. The dissociated neurons were plated at a density of approximately 1×10^5 ml^{-1}. After 6-h incubation at 37 °C in a humidified 5% CO_2, DMEM was replaced with the Neurobasal™-A medium supplemented with B-27 (Gibco). The cells in 6–8-day-old cultures were utilized in following intracellular calcium level detection.

2.6. Fluo-3 loading and intracellular calcium fluorescence measurement

The intracellular calcium level of hippocampal neurons was followed with a calcium-sensitive fluorescent dye Fluo-3 (Molecular Probes). The neurons grown on Petri-dishes were firstly incubated with 5 μM fluo-3-AM in HBSS solution at 37 °C for 28 min, and then were rinsed to remove exceeding fluo-3-AM and bathed in HBSS. The LCSM system Leica TCS-SP2 consisted of a TCS-SP2 laser scanning confocal unit interfaced with a Nikon Diaphot

inverted microscope equipped with a Nikon 20× Neofluor objective. The intracellular calcium fluorescent intensity was measured by scanning the specimen once every 3 s with a 488 nm line of a krypton–argon laser.

3. Results

3.1. Humanin peptides accelerate $A\beta_{1–40}$ aggregation

The time course of light-scattering intensity of $A\beta_{1–40}$, $A\beta_{1–40}$ + HN (1:2) and $A\beta_{1–40}$ + HNG (1:2) were recorded, respectively, and presented in Fig. 1. The intensity of $A\beta_{1–40}$ almost did not vary before the sixth day, but increased continually during the next 5 days. Both HN and HNG led quick rise of the light-scattering intensity of $A\beta_{1–40}$, and the average scattering intensity of $A\beta_{1–40}$ + HNG is almost 10 times of $A\beta_{1–40}$ + HN and $A\beta_{1–40}$ at maximum. The scattering intensity of $A\beta_{1–40}$, $A\beta_{1–40}$ + HN (1:2) and $A\beta_{1–40}$ + HNG (1:2) decreased quickly after 10- or 11-day incubation at 37 °C, respectively.

3.2. Effects of humanin peptides on $A\beta_{1–40}$ fibrogenesis

The morphological feature of $A\beta_{1–40}$, $A\beta_{1–40}$ + HN and $A\beta_{1–40}$ + HNG were revealed using transmission electron microscopy (TEM) and scanning electron microscopy (SEM), respectively, and presented in Figs. 2 and 3.

As a control, the $A\beta_{1–40}$ aggregate was investigated firstly. Small, short and twist assembled structure with diameters between 5 and 10 nm was observed using TEM before the sixth day, the morphological characteristics of which is consistent with that of “protofibrils” (Fig. 2a) [7,8]. After 6-day incubation, the long and smooth “mature” fibrils with diameter 7–10 nm were observed and became abundant with time going. Fig. 2b shows the morphological characteristics of $A\beta_{1–40}$ fibrils after 12-day incubation. Although HN can lead the light-scattering intensity increase quickly, $A\beta_{1–40}$ + HN showed similar morphological feature to $A\beta_{1–40}$ and the fibrillar structures were observed. Fig. 2c shows the morphological features of $A\beta_{1–40}$ + HN after 12-day incubation, the formed fibrils with diameter 10–15 nm, are thicker than $A\beta_{1–40}$ and tend to twist each other.

The nanoscale globular particles with diameters 50–250 nm are the morphological characteristics of $A\beta_{1–40}$ incubating with HNG over 6 h, as presented in Fig. 3a. So-called “rods” or fibers with diameter near 200 nm assembled by the particles were observed. The inset shows the stacked particles with well-proportioned diameters 150–200 nm. The quick nanoscale particles formation appears to be consistent with the quick increase of light-scattering intensity after adding HNG to $A\beta_{1–40}$. These indicate that the morphological characteristics of $A\beta_{1–40}$ + HNG are not feint caused by EM sample preparation. Because of the thick deposit formation of $A\beta_{1–40}$, it is difficult to disperse the sample and reveal the morphological in detail using TEM. With time going, the globular particles transformed to amorphous morphological characteristics. Fig. 3b shows the morphological characteristics of $A\beta_{1–40}$ + HNG after 12-day incubation, and the inset is a broad view of it.

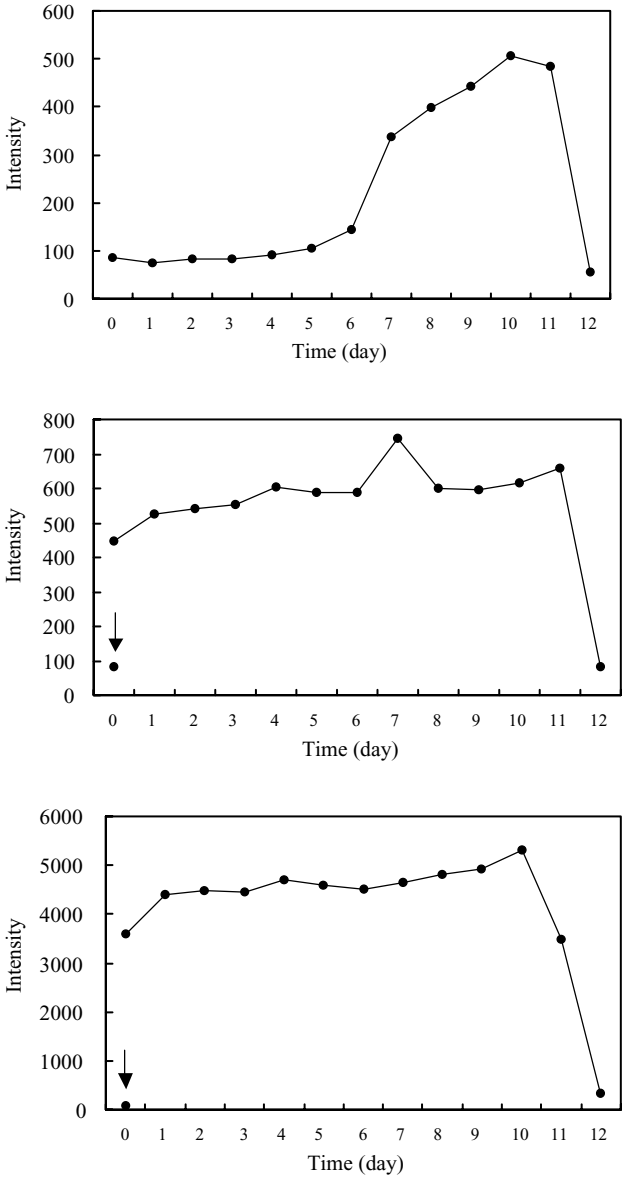

Fig. 1. The curves of light scattering of $A\beta_{1–40}$ (a), $A\beta_{1–40}$ + HN (b) and $A\beta_{1–40}$ + HNG (c) in PBSA, recorded at 37 °C, pH 7.2. In the experiments, the concentrations of $A\beta_{1–40}$ are the same (100 μM), the molar ratio of humanins/$A\beta_{1–40}$ is 2:1. The arrows in (b) and (c) indicate the intensity of the light scattering of $A\beta_{1–40}$ itself before adding HN or HNG.

3.3. Humanin peptides effects on $[Ca^{2+}]_i$ increasing caused by $A\beta_{1–40}$ aggregates

Usually, calcium influx is proposed as an initial event of Aβ-induced multiple events, since calcium chelation can prevent subsequent events, including reactive oxygen species generation and tau hyperphosphorylation. We followed the

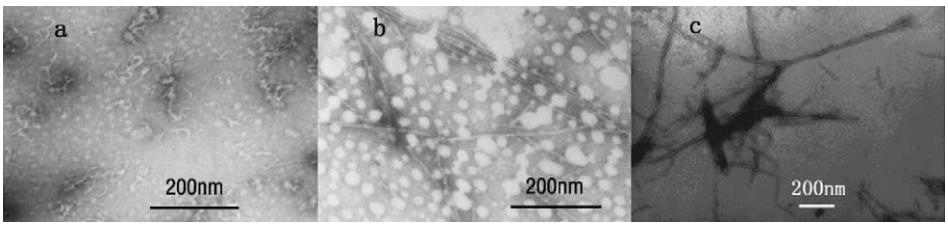

Fig. 2. The morphological characteristics of $A\beta_{1-40}$ and $A\beta_{1-40}$ + HN aggregation revealed by TEM. The short and twist $A\beta_{1-40}$-assembled structures with diameter 5–10 nm, termed "protofibrils", were found, the micrograph (a) in the sixth day shown. The smooth fibrils with diameters in 7–10 nm and lengths in several micrometers appeared after 6-day incubation, panel (b) presents the fibrils formed after 12 days. The fibrils with diameters 10–15 nm formed by $A\beta_{1-40}$ + HN after the 12-day incubation (c) are thicker in diameter than $A\beta_{1-40}$ fibrils, and they appeared to assemble. The concentration of $A\beta_{1-40}$ is 8.0 μM and the molar ratio of HN/$A\beta_{1-40}$ is 2:1. The micrographs of the negative stained peptide samples were taken with EM.

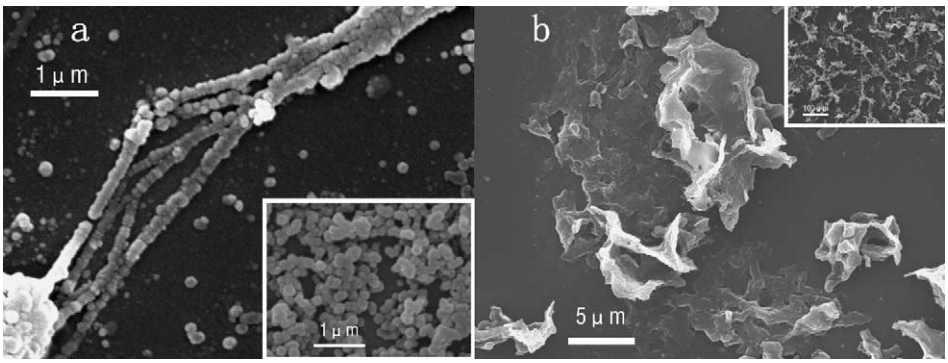

Fig. 3. The morphological characteristics of $A\beta_{1-40}$ + HNG aggregation were revealed with SEM. A large amount of nanoscale particles with diameters 50–200 nm formed in $A\beta_{1-40}$ + HNG after 6-h incubation was revealed, and the "rods" with diameter near 200 nm (a) formed by the particles assembly. The inset of panel (a) presents the particles with homologous diameter near 200 nm, which tend to stack. With time, a large amount of amorphous deposit appeared, the magnified micrograph (b) was taken after the 12-day incubation, and the inset presents the broad view. The concentration of $A\beta_{1-40}$ is 8.0 μM and the molar ratio of HNG/$A\beta_{1-40}$ is 2:1.

intracellular calcium level of neurons before and after adding specimens ($A\beta_{1-40}$, $A\beta_{1-40}$ + HN and $A\beta_{1-40}$ + HNG after 12-day incubation were used) as shown in Fig. 4. Fig. 4a–d represents the calcium intensity before 0 s and after 3, 30 and 300 s of adding fibrillar $A\beta_{1-40}$. Fig. 4e–h represents the calcium intensity before 0 s and after 3, 30 and 300 s of adding $A\beta_{1-40}$ + HN. Fig. 4i–l represents the calcium intensity before 0 s and after 3, 30 and 300 s of adding $A\beta_{1-40}$ + HNG. The accompanying histogram in the Fig. 4 shows analyses of ≥84 cells from four cultures each from independent experiments, in which 3.7% cells are insensitive to fibrillar $A\beta_{1-40}$ and 96.3% cells present calcium influx, 14.2 and 38.8% cells, subtracting $A\beta_{1-40}$-insensitive cells, were prohibited by HN and HNG, respectively, from $A\beta_{1-40}$-induced intracellular calcium increase.

4. Discussion

Humanin peptides could effectively abolish neuronal cell death caused by a wide spectrum of FAD genes and Aβ derivative as reported by Nishimoto and coworkers [9–11], but it is still uncertain how humanin peptides antagonize Aβ neurotoxicity and protect neurons, even though the evidence of receptor-mediated route was discovered [11]. Since Aβ fibrogenesis is very important for its neurotoxicity, to investigate Aβ morphological alteration triggered by humanins could reveal the neuro-protective mechanism of humanin peptides, including the relationship between Aβ and humanin peptides.

Although the mechanism of the Aβ fibrillization is not yet clear, it is usually suggested that amyloid fibrils formation is an ordered polymerization process characterized by a slow nucleation, followed by rapid growth step [7,15]. Because $A\beta_{1-40}$ HCl salt and TFA salt have different aggregating dynamic feature investigated by Kaneko et al. [12], the $A\beta_{1-40}$ peptide was treated with TFA to keep its homological chemical distribution prior to use in our experiment. As shown in Fig. 1a, the light-scattering intensity of $A\beta_{1-40}$ had almost no variance during the first 6 days, whereas the intensity increased instantly during the next 5-day incubation. TEM revealed that the short and twisted structures (Fig. 2a) with diameter near 5–10 nm were observed during the first 7 days, and the characteristics of which is consistent with the "protofibrils" suggested by Harper and coworkers [7,8]. These results suggest that the first 7-day incubation of $A\beta_{1-40}$ is consistent with the slow, intricate, so-called "seeding" or nucleation process of

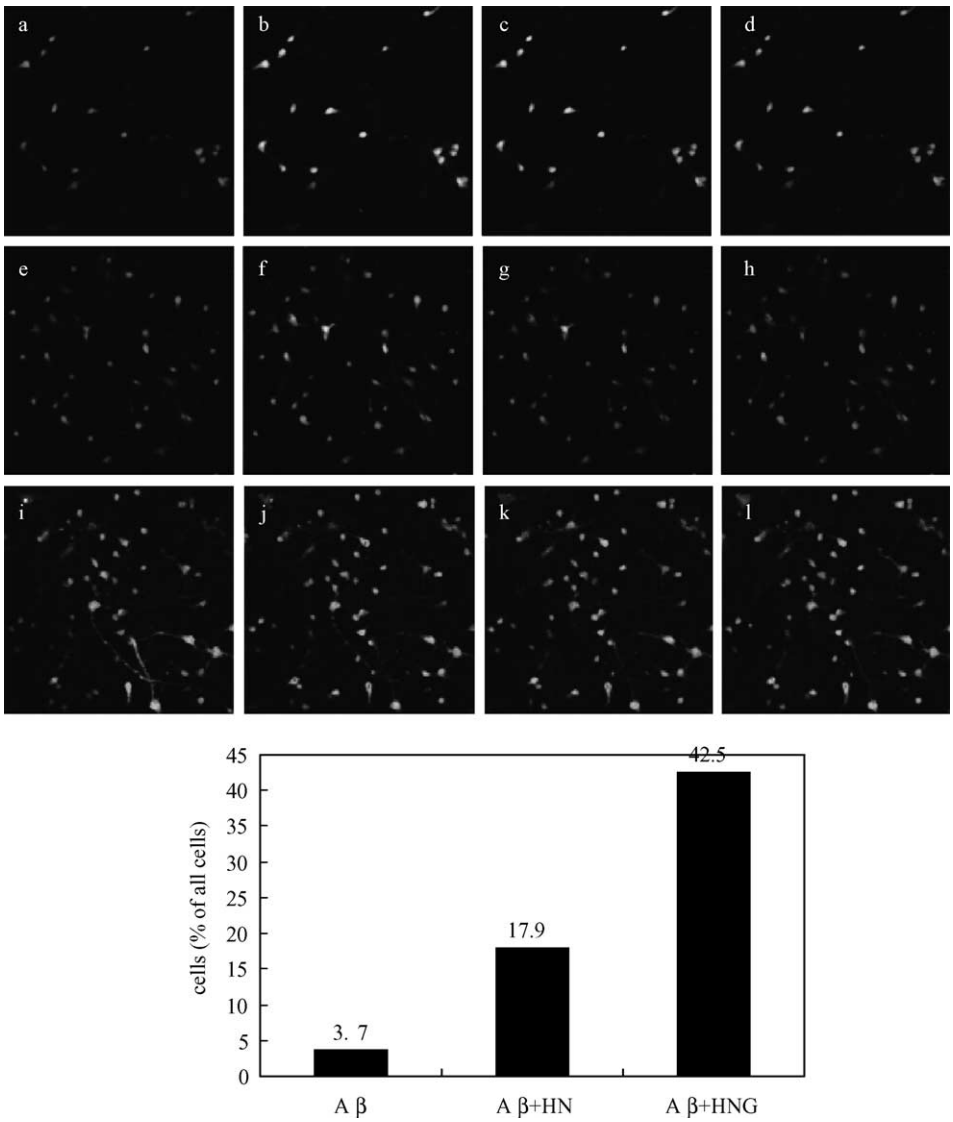

Fig. 4. HN and HNG present different potential suppressing $A\beta_{1–40}$-induced calcium influx of neurons, revealed with LSCM. Micrographs (a–d) represent the calcium intensity before 0 s and after 3, 30 and 300 s of adding fibrillar $A\beta_{1–40}$; (e–h) represent the calcium intensity before 0 s and after 3, 30 and 300 s of adding $A\beta_{1–40}$ + HN; (i–l) represent the calcium intensity before 0 s and after 3, 30 and 300 s of adding $A\beta_{1–40}$ + HNG. After subtracting $A\beta_{1–40}$-insensitive cells, HN and HNG could prohibit 14.2 and 38.8% $A\beta_{1–40}$-induced calcium influx of neurons. The analyses are from ≥84 cells of four cultures each from independent experiments. In the experiments, the concentrations of $A\beta_{1–40}$ are same (100 μM), the molar ratio of humanins/$A\beta_{1–40}$ is 2:1.

$A\beta_{1–40}$ fibrillization [15,16], in which conformational transition, oligomerization and seed formation exist. With the light-scattering intensity increasing from the sixth day, the fibrils with diameter near 10 nm appeared and became abundant revealed by TEM, which are interpreted as the formed "seed" triggered more fibrils formation and growth [15,16], in addition, the "seed" also induce more molecules to aggregate and form more nanoscale particles, which would induce the light-scattering intensity rise if the molecular aggregates can disperse well in solution.

It is a puzzle why the intensity decreased after 10- or 11-day incubation, as observed in $A\beta_{1–40}$, $A\beta_{1–40}$ + HN and $A\beta_{1–40}$ + HNG. A simple interpretation is a decrease of the total scattering area of particles in solution. As we know, light-scattering intensity correlates closely with the surface area of particles in solution, determined by particles size and number, the particles formed by oligomerization of soluble molecules can induce the increase in intensity. Since both fibrils growth (in $A\beta_{1–40}$ and $A\beta_{1–40}$ + HNG) and particles aggregation (in $A\beta_{1–40}$ + HNG) will reduce particles number and or increase particle size, the consequence is decreasing the efficient surface area, which would finally lead the light-scattering intensity decrease.

Compared with $A\beta_{1–40}$, both HN and HNG induced a strong and quick light-scattering intensity increase of $A\beta_{1–40}$ when added to $A\beta_{1–40}$ solution, respectively

(Fig. 1b and c). The intensity persisted at a high level during incubation and decreased quickly beginning at the 10th or 11th day. We found that the average intensity of $A\beta_{1-40}$ + HNG before the 10th day is almost 10 times stronger than that of $A\beta_{1-40}$ at the 11th day. HN caused a similar rise in intensity to $A\beta_{1-40}$ at the 11th day. These appear to be consistent with the quick and abundant globular particles formation of $A\beta_{1-40}$ + HNG (Fig. 3a), which will induce strong light-scattering signals.

Although HN led an obvious alteration of $A\beta_{1-40}$ aggregation dynamics revealed by light scattering, electron microscopy revealed that HN did not lead to obvious morphological alteration of $A\beta_{1-40}$, except that the fibrils diameter 10–15 nm (Fig. 2c) are thicker than that of $A\beta_{1-40}$. It is difficult to explain in detail how HN affects $A\beta_{1-40}$ fibrogenesis, based on the present study. However this result confirms the interaction between $A\beta_{1-40}$ and HN, which could affect $A\beta_{1-40}$ molecular assembly in solution. Compared with HN, HNG caused completely different morphological characteristics of $A\beta_{1-40}$, as shown in Fig. 3. A large amount of nanoscale particles with diameters between 50 and 250 nm formed quickly after adding HNG (Fig. 3a), which could interpret the strong light-scattering intensity increase, as shown in the time-course of light-scattering intensity of $A\beta_{1-40}$ + HNG aggregation (Fig. 1c). The homogenous globular particles (Fig. 3a, inset) and the nanoscale fibers with diameters 150–200 nm assembled by the particles (Fig. 3a) were found, and are unlikely to arise from the sample preparation of electron microscopy, indicating that the HNG interaction with $A\beta_{1-40}$ led to the nanoscale particles formation at the beginning of aggregation. A large amount of amorphous deposit was observed (Fig. 3b) with time, but, unfortunately, we did not observe the transformation intermediates from the globular to the amorphous.

Although more than five to six kinds of time-course patterns of intracellular calcium alteration in fluorescent intensity were observed (not shown, for instance, oscillation, quick rise, slow rise), and humanin peptides could also alter the percent of cells presenting different calcium alteration patterns, we simply compartmentalized them into a sensitive pattern with intracellular calcium increase and an insensitive pattern, since it is uncertain why fibrillar $A\beta_{1-40}$ can induce such different patterns of intracellular calcium alteration and how each of the patterns associates with cellular apoptosis. Regardless of the multiple events triggered by Aβ, it is generally considered that Aβ-induced toxicity is associated with a disturbance of cellular membrane stability and cellular calcium channel. HNG-induced morphological alteration of $A\beta_{1-40}$ presents a weaker potential of intracellular calcium influx than the fibrillar $A\beta_{1-40}$, suggesting that HNG interaction partially prohibits $A\beta_{1-40}$ from forming “toxic ultrastructures”, which affect cells by binding cellular receptor, disturbing membrane stability or forming cationic channel [14,17,21].

It has been suggested, based on the evidence that the effective concentration of HNG is lower by three to four orders than the toxic concentration of $A\beta_{1-40}$, that humanin peptides suppress $A\beta_{1-40}$-induced neurotoxicity through an indirect interaction [11]. In addition, evidence tends to confirm a specific binding site(s) of humanin peptides-associating F11 cells [11]. In this work, we used preformed aggregates of $A\beta_{1-40}$–humanins interactions to examine intracellular calcium level of neurons, which is helpful of revealing neuron-protection activity of humanin peptides through interaction with $A\beta_{1-40}$ other than cellular receptor or other routes. Evidence confirmed the humanin interactions with $A\beta_{1-40}$, in which, we increased molar ratio of humanin peptides to 2:1 (humanins/$A\beta_{1-40}$), (a) humanin peptides affect $A\beta_{1-40}$ aggregation dynamics, (b) HNG changes the $A\beta_{1-40}$ morphological feature obviously, (c) and HNG interactions with $A\beta_{1-40}$ partially suppress $A\beta_{1-40}$-induced calcium influx. The different conclusions mean that humanin peptides could exert different approaches to protect neurons, expected for their potential of binding special molecules on cell membranes. Therefore, our work confirmed that HNG can affect $A\beta_{1-40}$ fibrogenesis and $A\beta_{1-40}$-induced calcium influx, and helps clarify the multiple roles and structural mechanism of humanin peptides protecting neurons.

Acknowledgments

The project financially supported by Natural Science Foundation of China (20103001, 20273002).

References

[1] Arispe N, Rojas E, Pollard HB. Alzheimer disease amyloid beta protein forms calcium channels in bilayer membranes: blockade by tromethamine and aluminium. Proc Natl Acad Sci USA 1993;90:567–71.
[2] Brewer GJ. Isolation and culture of adult rat hippocampal neurons. J Neurosci Methods 1997;71:143–55.
[3] Carrell RW, Lomas DA. Conformational disease. Lancet 1997;350: 134–8.
[4] Fields GB, Noble RL. Solid phase peptide synthesis utilizing 9-fluorenylmethoxy-carbonyl amino acids. Int J Pept Protein Res 1990;35:161–214.
[5] Gearing M, Mori H, Mira S. Aβ-peptide length and apolipoprotein E genotype in Alzheimer’s disease. Ann Neurol 1996;39:395–9.
[6] Hardy JA, Higgins GA. Alzheimer’s disease: the amyloid cascade hypothesis. Science 1992;256:184–5.
[7] Harper JD, Lansbury Jr PT. Models of amyloid seeding in Alzheimer’s disease and scrapie: mechanistic truths and physiological consequences of the time-dependent solubility of amyloid proteins. Annu Rev Biochem 1997;66:385–407.
[8] Harper JD, Wong SS, Lieber CM, Lansbury PT. Observation of metastable Aβ amyloid protofibrils by atomic force microscopy. Chem Biol 1997;4:119–25.
[9] Hashimoto Y, Ito Y, Niikura T, Shao ZJ, Hata M, Oyama F, Nishimoto I. Mechanism of neuroprotection by a novel resue factor humanin from Swedish mutant amyloid precursor protein. Biochem Biophys Res Commun 2001;83:460–8.
[10] Hashimoto Y, Niikura T, Ito Y, Sudo H, Hata M, Arakawa E, Abe Y, Kita Y, Nishimoto I. Detailed characterization of neuroprotection by a resue factor humanin against various Alzheimer’s disease-relevant insults. J Neurosci 2001;21:9235–45.

[11] Hashimoto Y, Niikura T, Tajima H, Yasukawa T, Sudo H, Ito Y, Kita Y, Kawasumi M, Kouyama K, Doyu M, Sobue G, Koidek T, Tsuji S, Lang J, Kurokawa K, Nishimoto I. A rescue factor abolishing neuronal cell death by a wide spectrum of familial Alzheimer's disease genes and Aβ. Proc Natl Acad Sci USA 2001;98:6336–41.
[12] Kaneko I, Yamada N, Sakuraba Y, Kamenosono M, Tutumi S. Suppression of mitochondrial succinate dehydrogenase, a primary target of beta-amyloid, and its derivative racemized at Ser residue. J Neurochem 1995;65:2585–93.
[13] Katzman R, Kawas C. The epidemiology of dementia and Alzheimer disease. In: Terry RD, Katzman R, Bick KL, editors. Alzheimer disease. New York: Raven Press; 1994. p. 105.
[14] Kawahara M, Kuroda Y. Molecular mechanism of neurodegeneration induced by Alzheimer's β-amyloid protein: channel formation and disruption of calcium homeostasis. Brain Res Bull 2000;4:389–97.
[15] Lomakin A, Chung DS, Benedek GB, Kirschner DA, Teplow DB. On the nucleation and growth of amyloid β-protein fibrils: detection of nuclei and quantitation of rate constants. Proc Natl Acad Sci USA 1996;93:1125–9.
[16] Lomakin A, Teplow DB, Kirschner DA, Benedek GB. Kinetic theory of fibrillogenesis of amyloid β-protein. Proc Natl Acad Sci USA 1997;94:7942–7.
[17] Ma XC, Sha YL, Lin KC, Nie SQ. The effect of fibrillar $A\beta_{1-40}$ on membrane fluidity and permeability. Protein Pept Lett 2002;9: 173–8.
[18] Mattson MP, Cheng B, Davis D, Bryant K, Lieberburg I, Rydel RE. β-Amyloid peptides destabilize calcium homeostasis and render human cortical neurons vulnerable to excitotoxicity. J Neurosci 1992;12:376–89.
[19] Selkoe DJ. The molecular pathology of Alzheimer's disease. Neuron 1991;6:487–98.
[20] Seubert P, Oltersdorf T, Lee MG, Barbour R, Blomquist C, Davis DL, et al. Secretion of β-amyloid precursor protein cleaved at the amino terminus of the β-amyloid peptide. Nature 1993;361: 260–3.
[21] Yan SD, Chen X, Fu J, Chen M, Zhu H, Roher A, et al. RAGE and amyloid-β peptide neurotoxicity in Alzheimer's disease. Nature 1996;382:685–91.
[22] Zagorski MG, Yang J, Shao H, Ma K, Zeng H, Hong A. Methodological and chemical factors affecting amyloid β peptide amyloidogenicity. In: Colowick SP, Kaplan NO, editors. Methods in enzymology, vol. 309. New York: Academic Press; 1999. p. 189–204.